Steel and Composite Structures, *Vol. 17*, *No. 1* (*2014*) *21-46*
DOI: http://dx.doi.org/10.12989/scs.2014.17.1.021

A *n*-order four variable refined theory for bending and free vibration of functionally graded plates

I. Klouche Djedid [1,2], Abdelkader Benachour [1], Mohammed Sid Ahmed Houari [3], Abdelouahed Tounsi [*1,3] and Mohammed Ameur [3,4]

[1] *Material and Hydrology Laboratory*, *University of Sidi Bel Abbes*, *Faculty of Technology*, *Civil Engineering Department*, *Algeria*
[2] *Université Ibn Khaldoun*, *BP 78 Zaaroura*, *14000 Tiaret*, *Algeria*
[3] *Laboratoire des Structures et Matériaux Avancés dans le Génie Civil et Travaux Publics*, *Université de Sidi Bel Abbes*, *Faculté de Technologie*, *Algeria*
[4] *Ecole Nationale Polytechnique d'Oran*, *Algeria*

(*Received August 19*, *2013*, *Revised January 14*, *2014*, *Accepted February 02*, *2014*)

Abstract. This paper presents a simple *n*-order four variable refined theory for the bending and vibration analyses of functionally graded plates. By dividing the transverse displacement into bending and shear parts, the number of unknowns and governing equations of the present theory is reduced, and hence, makes it simple to use. The present theory is variationally consistent, uses the *n*-order polynomial term to represent the displacement field, does not require shear correction factor, and gives rise to transverse shear stress variation such that the transverse shear stresses vary parabolically across the thickness satisfying shear stress free surface conditions. The governing equations are derived by employing the Hamilton's principle and the physical neutral surface concept. The accuracy of the present solutions is verified by comparing the obtained results with available published ones.

Keywords: *n*th-order four variable refined theory; FG plates; vibration; bending; neutral surface position

1. Introduction

Composite materials have been successfully used in aircraft and other engineering applications for many years because of their excellent strength to weight and stiffness to weight ratios. Recently, advanced composite materials known as functionally graded material have attracted much attention in many engineering applications due to their advantages of being able to resist high temperature gradient while maintaining structural integrity (Koizumi 1997). The functionally graded materials (FGMs) are microscopically inhomogeneous, in which the mechanical properties vary smoothly and continuously from one surface to the other. They are usually made from a mixture of ceramics and metals to attain the significant requirement of material properties.

*Corresponding author, Professor, E-mail: tou_abdel@yahoo.com

http://www.techno-press.org/?journal=scs&subpage=8 ISSN: 1229-9367 (Print), 1598-6233 (Online)

Due to the increased relevance of the FGMs structural components in the design of engineering structures, many studies have been reported on the static, and vibration analyses of functionally graded (FG) plates. Reddy (2000) presented theoretical formulation and finite element models based on third order shear deformation theory for static and dynamic analysis of the FG plates. Batra and Jin (2005) used the first-order shear deformation theory coupled with the finite element method to study the free vibrations of rectangular anisotropic FG plate. Zenkour (2006) investigated the bending response of simply supported FG plate using a generalized shear deformation plate theory. Abrate (2006) analyzed the problems of free vibrations, buckling, and static deflections of the FG plates. Chi and Chung (2006a, b) studied the mechanical behaviour of FG plates under transverse load. Three evaluations were considered for the FGM properties, which include power-law, sigmoid or exponential function. Matsunaga (2008) calculated the natural frequencies and buckling stresses of plates made of functionally graded materials (FGMs) using a 2-D higher-order deformation theory. Chen *et al*. (2008, 2009) carried out the vibration and stability of FG plates based on different plate theories. Lü *et al*. (2009a) presented a semi-analytical 3-D elasticity solutions for orthotropic multi-directional functionally graded plates using the differential quadrature method (DQM) based on the state-space formalism. Lü *et al*. (2009b) studied the free vibration of FG thick plates on Pasternak foundation using 3-D exact solutions.The second-order shear deformation theory is successfully applied Shahrjerdi *et al*. (2010) to present the displacements field in solar functionally graded plate with simply support conditions subjected to a different type of mechanical loadings such as sinusoidal and uniform distributed loads. Bodaghi and Saidi (2010) presented analytical approach based on a HOST to determine critical buckling loads of thick FG rectangular plates. Talha and Singh (2010) investigated the free vibration and static analysis of functionally graded plates using the finite element method by employing a higher order shear deformation theory. Xiang *et al*. (2011) proposed a *n*-order shear deformation theory for free vibration of functionally graded and composite sandwich plates. Using the sinusoidal shear deformation theory, Sobhy (2013) studied the vibration and buckling behavior of exponentially graded sandwich plate resting on elastic foundations under various boundary conditions. Yaghoobi and Torabi (2013) studied the thermal buckling of FG plates resting on two-parameter Pasternak's foundations by using the first-order shear deformation plate theory. Yaghoobi and Yaghoobi (2013) proposed an analytical investigation on the buckling analysis of symmetric sandwich plates with FG face sheets resting on an elastic foundation based on the first-order shear deformation plate theory and subjected to mechanical, thermal and thermo-mechanical loads. However, various higher order shear deformation theories are developed using five or more unknown functions. Recently, Tounsi and his co-workers (Hadji *et al*. 2011, Houari *et al*. 2011, Bourada *et al*. 2012, Bachir Bouiadjra *et al*. 2012, Fekrar *et al*. 2012, Fahsi *et al*. 2012, Bouderba *et al*. 2013) developed new higher order plates theories involving only four unknown functions.

In this paper, a *n*-order four variable refined theory is used to analyze the static and vibration characteristics of functionally graded plates. The present *n*-order four variable refined theory is based on assumption that the in-plane and transverse displacements consist of bending and shear components, in which the bending components do not contribute toward shear forces and, likewise, the shear components do not contribute toward bending moments. The most interesting feature of this theory is that it accounts for a parabolic variation of the transverse shear strains across the thickness and satisfies the zero traction boundary conditions on the top and bottom surfaces of the plate without using shear correction factors. The material properties of FG plate are assumed to vary according to a power law distribution of the volume fraction of the constituents. To simplify

the governing equations for the FG plates, the coordinate system is located at the physical neutral surface of the plate. This is due to the fact that the stretching – bending coupling in the constitutive equations of an FG plate does not exist when the physical neutral surface is considered as a coordinate system (Zhang and Zhou 2008, Yahoobi and Feraidoon 2010, Ould Larbi *et al*. 2013, Bouremana *et al*. 2013). Thus, the present *n*-order four variable refined theory based on the exact position of neutral surface together with Hamilton principle are employed to extract the motion equations of the FG plates. Analytical solutions are obtained for simply supported plate, and its accuracy is verified by comparing the obtained results with those reported in the literature.

2. Mathematical formulation

Consider a rectangular plate made of FGMs of thickness h, length a, and width b, referred to the rectangular Cartesian coordinates (x, y, z). Since in functionally graded plates the condition of mid-plane symmetry does not exist, the stretching and bending equations are coupled. But, if the origin of the coordinate system is suitably selected in the thickness direction of the FG plate so as to be the neutral surface, the analysis of the FG plates can easily be treated with the homogenous isotropic plate theories, because the stretching and bending equations of the plate are not coupled. In order to determine the position of neutral surface of FG plates, two different datum planes are considered for the measurement of z, namely, z_{ms} and z_{ns} measured from the middle surface and the neutral surface of the plate, respectively, as shown in Fig. 1. Following the power law distribution in the thickness direction, the volume fractions of ceramic constituent V_C, and metal constituent V_M, may be written in the form

$$V_C = \left(\frac{z_{ms}}{h} + \frac{1}{2}\right)^k = \left(\frac{z_{ns} + C}{h} + \frac{1}{2}\right)^k \tag{1}$$

Material non-homogeneous properties of a functionally graded material plate may be obtained by means of the Voigt rule of mixture (Suresh and Mortensen 1998). Thus, using Eq. (1), the material non-homogeneous properties of FG plate P, as a function of thickness coordinate, become

$$P(z) = P_M + P_{CM}\left(\frac{z_{ns} + C}{h} + \frac{1}{2}\right)^k, \quad P_{CM} = P_C - P_M \tag{2}$$

where P_M and P_C are the corresponding properties of the metal and ceramic, respectively, and k is the material parameter which takes the value greater or equal to zero. Also, the parameter C is the distance of neutral surface from the middle surface. In the present work, we assume that the elasticity modules E is described by Eq. (2), while Poisson's ratio v, is considered to be constant across the thickness. The position of the neutral surface of the FG plate is determined to satisfy the first moment with respect to Young's modulus being zero as follows (Ould Larbi *et al*. 2013, Bouremana *et al*. 2013)

$$\int_{-h/2}^{h/2} E(z_{ms})(z_{ms} - C)dz_{ms} = 0 \tag{3}$$

Consequently, the position of neutral surface can be obtained as

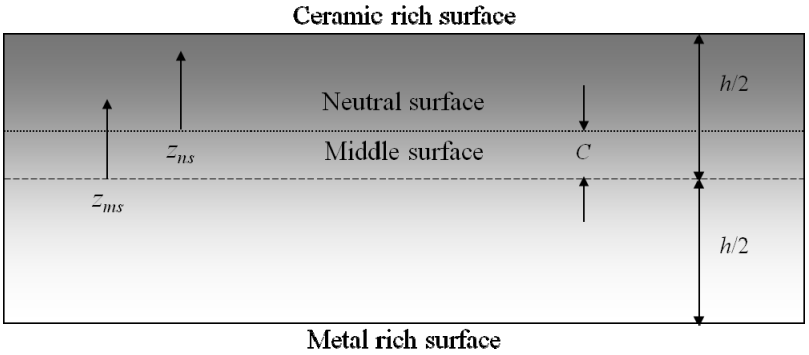

Fig. 1 The position of middle surface and neutral surface for a functionally graded plate

$$C = \frac{\int_{-h/2}^{h/2} E(z_{ms}) z_{ms} dz_{ms}}{\int_{-h/2}^{h/2} E(z_{ms}) dz_{ms}} \tag{4}$$

It is clear that the parameter C is zero for homogeneous isotropic plates, as expected.

2.1 Basic assumptions

The assumptions of the present theory are as follows:

(1) The origin of the Cartesian coordinate system is taken at the neutral surface of the FG plate.
(2) The displacements are small in comparison with the plate thickness and, therefore, strains involved are infinitesimal.
(3) The transverse displacement w includes two components of bending w_b and shear w_s. Both these components are functions of coordinates x, y, and time t only.

$$w(x, y, z_{ns}, t) = w_b(x, y, t) + w_s(x, y, t) \tag{5}$$

(4) The displacements u in x-direction and v in y-direction consist of extension, bending, and shear components.

$$u = u_0 + u_b + u_s, \quad v = v_0 + v_b + v_s \tag{6}$$

The bending components u_b and v_b are assumed to be similar to the displacements given by the classical plate theory. Therefore, the expression for u_b and v_b can be given as

$$u_b = -z_{ns} \frac{\partial w_b}{\partial x}, \quad v_b = -z_{ns} \frac{\partial w_b}{\partial y} \tag{7}$$

The shear components u_s and v_s give rise, in conjunction with w_s, to the sinusoidal variations of

shear strains γ_{xz}, γ_{yz} and hence to shear stresses τ_{xz}, τ_{yz} through the thickness of the plate in such a way that shear stresses τ_{xz}, τ_{yz} are zero at the top and bottom faces of the plate. Consequently, the expression for u_s and v_s can be given as

$$u_s = -f(z_{ns})\frac{\partial w_s}{\partial x}, \quad v_s = -f(z_{ns})\frac{\partial w_s}{\partial y} \tag{8}$$

where

$$f(z_{ns}) = \frac{1}{n}\left(\frac{2}{h}\right)^{n-1}(z_{ns}+C)^n \tag{9}$$

2.2 Kinematics and constitutive equations

Based on the assumptions made in the preceding section, the displacement field of the *n*-order four variable refined theory can be obtained using Eqs. (5)-(9) as

$$u(x,y,z_{ns},t) = u_0(x,y,t) - z_{ns}\frac{\partial w_b}{\partial x} - \frac{1}{n}\left(\frac{2}{h}\right)^{n-1}(z_{ns}+C)^n\frac{\partial w_s}{\partial x} \tag{10a}$$

$$v(x,y,z_{ns},t) = v_0(x,y,t) - z_{ns}\frac{\partial w_b}{\partial y} - \frac{1}{n}\left(\frac{2}{h}\right)^{n-1}(z_{ns}+C)^n\frac{\partial w_s}{\partial y} \tag{10b}$$

$$w(x,y,z_{ns},t) = w_b(x,y,t) + w_s(x,y,t) \tag{10c}$$

The kinematic relations can be obtained as follows

$$\begin{Bmatrix}\varepsilon_x\\ \varepsilon_y\\ \gamma_{xy}\end{Bmatrix} = \begin{Bmatrix}\varepsilon_x^0\\ \varepsilon_y^0\\ \gamma_{xy}^0\end{Bmatrix} + z_{ns}\begin{Bmatrix}k_x^b\\ k_y^b\\ k_{xy}^b\end{Bmatrix} + f(z_{ns})\begin{Bmatrix}k_x^s\\ k_y^s\\ k_{xy}^s\end{Bmatrix}, \quad \begin{Bmatrix}\gamma_{yz}\\ \gamma_{xz}\end{Bmatrix} = g(z_{ns})\begin{Bmatrix}\gamma_{yz}^0\\ \gamma_{xz}^0\end{Bmatrix} \tag{11}$$

where

$$\begin{Bmatrix}\varepsilon_x^0\\ \varepsilon_y^0\\ \gamma_{xy}^0\end{Bmatrix} = \begin{Bmatrix}\dfrac{\partial u_0}{\partial x}\\ \dfrac{\partial v_0}{\partial y}\\ \dfrac{\partial u_0}{\partial y}+\dfrac{\partial v_0}{\partial x}\end{Bmatrix}, \quad \begin{Bmatrix}k_x^b\\ k_y^b\\ k_{xy}^b\end{Bmatrix} = \begin{Bmatrix}-\dfrac{\partial^2 w_b}{\partial x^2}\\ -\dfrac{\partial^2 w_b}{\partial y^2}\\ -2\dfrac{\partial^2 w_b}{\partial x\partial y}\end{Bmatrix}, \quad \begin{Bmatrix}k_x^s\\ k_y^s\\ k_{xy}^s\end{Bmatrix} = \begin{Bmatrix}-\dfrac{\partial^2 w_s}{\partial x^2}\\ -\dfrac{\partial^2 w_s}{\partial y^2}\\ -2\dfrac{\partial^2 w_s}{\partial x\partial y}\end{Bmatrix}, \quad \begin{Bmatrix}\gamma_{yz}^0\\ \gamma_{xz}^0\end{Bmatrix} = \begin{Bmatrix}\dfrac{\partial w_s}{\partial y}\\ \dfrac{\partial w_s}{\partial x}\end{Bmatrix}, \tag{12a}$$

and

$$g(z_{ns}) = 1 - \frac{df(z_{ns})}{dz_{ns}} = 1 - \frac{(z_{ns}+C)^n}{(z_{ns}+C)}\left(\frac{2}{h}\right)^{n-1} \tag{12b}$$

For elastic and isotropic FGMs, the constitutive relations can be written as

$$\begin{Bmatrix}\sigma_x\\ \sigma_y\\ \tau_{xy}\end{Bmatrix}=\begin{bmatrix}Q_{11} & Q_{12} & 0\\ Q_{12} & Q_{22} & 0\\ 0 & 0 & Q_{66}\end{bmatrix}\begin{Bmatrix}\varepsilon_x\\ \varepsilon_y\\ \gamma_{xy}\end{Bmatrix} \text{ and } \begin{Bmatrix}\tau_{yz}\\ \tau_{zx}\end{Bmatrix}=\begin{bmatrix}Q_{44} & 0\\ 0 & Q_{55}\end{bmatrix}\begin{Bmatrix}\gamma_{yz}\\ \gamma_{zx}\end{Bmatrix} \tag{13}$$

where (σ_x, σ_y, τ_{xy}, τ_{yz}, τ_{yx}) and (ε_x, ε_y, γ_{xy}, γ_{yz}, γ_{xz}) are the stress and strain components, respectively. Using the material properties defined in Eq. (2), stiffness coefficients, Q_{ij}, can be expressed as

$$Q_{11}=Q_{22}=\frac{E(z_{ns})}{1-\nu^2}, \tag{14a}$$

$$Q_{12}=\frac{\nu\,E(z_{ns})}{1-\nu^2}, \tag{14b}$$

$$Q_{44}=Q_{55}=Q_{66}=\frac{E(z_{ns})}{2(1+\nu)}, \tag{14c}$$

2.3 Governing equations

Hamilton's principle is used herein to derive equations of motion. The principle can be stated in an analytical form as

$$0=\int_0^T\left(\delta U+\delta V-\delta K\right)dt \tag{15}$$

where δU is the variation of strain energy; δV is the variation of work done by external forces; and δK is the variation of kinetic energy. The variation of strain energy is calculated by

$$\begin{aligned}\delta U&=\int_\Omega\int_{-\frac{h}{2}-C}^{\frac{h}{2}-C}\left[\sigma_x\delta\varepsilon_x+\sigma_y\delta\varepsilon_y+\tau_{xy}\delta\gamma_{xy}+\tau_{yz}\delta\gamma_{yz}+\tau_{xz}\delta\gamma_{xz}\right]dz_{ns}d\Omega\\&=\int_\Omega\Big[N_x\delta\varepsilon_x^0+N_y\delta\varepsilon_y^0+N_{xy}\delta\varepsilon_{xy}^0+M_x^b\delta k_x^b+M_y^b\delta k_y^b+M_{xy}^b\delta k_{xy}^b+M_x^s\delta k_x^s\\&\quad+M_y^s\delta k_y^s+M_{xy}^s\delta k_{xy}^s+S_{yz}^s\delta\gamma_{yz}^s+S_{xz}^s\delta\gamma_{xz}^s\Big]d\Omega\end{aligned} \tag{16}$$

where Ω is the top surface and N, M, and S are stress resultants defined by

$$\begin{Bmatrix}N_x, & N_y, & N_{xy}\\ M_x^b, & M_y^b, & M_{xy}^b\\ M_x^s, & M_y^s, & M_{xy}^s\end{Bmatrix}=\int_{-\frac{h}{2}-C}^{\frac{h}{2}-C}\left(\sigma_x,\sigma_y,\tau_{xy}\right)\begin{Bmatrix}1\\ z_{ns}\\ f(z_{ns})\end{Bmatrix}dz_{ns}, \tag{17a}$$

$$\left(S_{xz}^{s}, S_{yz}^{s}\right)=\int_{-\frac{h}{2}-C}^{\frac{h}{2}-C}\left(\tau_{xz}, \tau_{yz}\right) g(z_{ns}) dz_{ns}. \tag{17b}$$

The variation of work done by external forces can be expressed as

$$\delta V=-\int_{\Omega} q\left(\delta w_b+\delta w_b\right) d\Omega \tag{18}$$

where q is the transverse load.

The variation of kinetic energy can be written as

$$\begin{aligned}
\delta K &= \int_{-\frac{h}{2}-C}^{\frac{h}{2}-C}\int_{\Omega}\left[\dot{u}\delta\dot{u}+\dot{v}\delta\dot{v}+\dot{w}\delta\dot{w}\right]\rho(z_{ns})\, d\Omega\, dz_{ns} \\
&= \int_{A}\left\{I_0\left[\dot{u}_0\delta\dot{u}_0+\dot{v}_0\delta\dot{v}_0+\left(\dot{w}_b+\dot{w}_s\right)\left(\delta\dot{w}_b+\delta\dot{w}_s\right)\right]\right. \\
&\quad -I_1\left(\dot{u}_0\frac{\partial\delta\dot{w}_b}{\partial x}+\frac{\partial\dot{w}_b}{\partial x}\delta\dot{u}_0+\dot{v}_0\frac{\partial\delta\dot{w}_b}{\partial y}+\frac{\partial\dot{w}_b}{\partial y}\delta\dot{v}_0\right) \\
&\quad -J_1\left(\dot{u}_0\frac{\partial\delta\dot{w}_s}{\partial x}+\frac{\partial\dot{w}_s}{\partial x}\delta\dot{u}_0+\dot{v}_0\frac{\partial\delta\dot{w}_s}{\partial y}+\frac{\partial\dot{w}_s}{\partial y}\delta\dot{v}_0\right) \\
&\quad +I_2\left(\frac{\partial\dot{w}_b}{\partial x}\frac{\partial\delta\dot{w}_b}{\partial x}+\frac{\partial\dot{w}_b}{\partial y}\frac{\partial\delta\dot{w}_b}{\partial y}\right)+K_2\left(\frac{\partial\dot{w}_s}{\partial x}\frac{\partial\delta\dot{w}_s}{\partial x}+\frac{\partial\dot{w}_s}{\partial y}\frac{\partial\delta\dot{w}_s}{\partial y}\right) \\
&\quad \left.+J_2\left(\frac{\partial\dot{w}_b}{\partial x}\frac{\partial\delta\dot{w}_s}{\partial x}+\frac{\partial\dot{w}_s}{\partial x}\frac{\partial\delta\dot{w}_b}{\partial x}+\frac{\partial\dot{w}_b}{\partial y}\frac{\partial\delta\dot{w}_s}{\partial y}+\frac{\partial\dot{w}_s}{\partial y}\frac{\partial\delta\dot{w}_b}{\partial y}\right)\right\} d\Omega
\end{aligned} \tag{19}$$

where dot-superscript convention indicates the differentiation with respect to the time variable t; and $(I_0, I_1, J_1, I_2, J_2, K_2)$ are mass inertias defined as

$$\left(I_0, I_1, J_1, I_2, J_2, K_2\right)=\int_{-\frac{h}{2}-C}^{\frac{h}{2}-C}\left(1, z_{ns}, f, z_{ns}^2, z_{ns}\, f, f^2\right)\rho(z_{ns}) dz_{ns} \tag{20}$$

Substituting the expressions for δU, δV, and δK from Eqs. (16), (18), and (19) into Eq. (15) and integrating by parts, and collecting the coefficients of δu_0, δv_0, δw_b, and δw_s, one obtains the following equations of motion

$$\begin{aligned}
\delta u_0: \quad & \frac{\partial N_x}{\partial x}+\frac{\partial N_{xy}}{\partial y}=I_0\ddot{u}_0-I_1\frac{\partial\ddot{w}_b}{\partial x}-J_1\frac{\partial\ddot{w}_s}{\partial x} \\
\delta v_0: \quad & \frac{\partial N_{xy}}{\partial x}+\frac{\partial N_y}{\partial y}=I_0\ddot{v}_0-I_1\frac{\partial\ddot{w}_b}{\partial y}-J_1\frac{\partial\ddot{w}_s}{\partial y}
\end{aligned} \tag{21}$$

$$\begin{aligned}
\delta w_b:\ & \frac{\partial^2 M_x^b}{\partial x^2}+2\frac{\partial^2 M_{xy}^b}{\partial x\partial y}+\frac{\partial^2 M_y^b}{\partial y^2}+q \\
&= I_0\left(\ddot{w}_b+\ddot{w}_s\right)+I_1\left(\frac{\partial \ddot{u}_0}{\partial x}+\frac{\partial \ddot{v}_0}{\partial y}\right)-I_2\nabla^2\ddot{w}_b-J_2\nabla^2\ddot{w}_s \\
\delta w_s:\ & \frac{\partial^2 M_x^s}{\partial x^2}+2\frac{\partial^2 M_{xy}^s}{\partial x\partial y}+\frac{\partial^2 M_y^s}{\partial y^2}+\frac{\partial S_{xz}^s}{\partial x}+\frac{\partial S_{yz}^s}{\partial y}+q \\
&= I_0\left(\ddot{w}_b+\ddot{w}_s\right)+J_1\left(\frac{\partial \ddot{u}_0}{\partial x}+\frac{\partial \ddot{v}_0}{\partial y}\right)-J_2\nabla^2\ddot{w}_b-K_2\nabla^2\ddot{w}_s
\end{aligned} \tag{21}$$

Using Eq. (9) in Eq. (13), and the subsequent results into Eq. (17), the stress resultants are obtained as

$$\begin{Bmatrix} N \\ M^b \\ M^s \end{Bmatrix}=\begin{bmatrix} A & 0 & B^s \\ 0 & D & D^s \\ B^s & D^s & H^s \end{bmatrix}\begin{Bmatrix} \varepsilon \\ k^b \\ k^s \end{Bmatrix},\quad S=A^s\gamma, \tag{22}$$

where

$$N=\left\{N_x,N_y,N_{xy}\right\}^t,\quad M^b=\left\{M_x^b,M_y^b,M_{xy}^b\right\}^t,\quad M^s=\left\{M_x^s,M_y^s,M_{xy}^s\right\}^t, \tag{23a}$$

$$\varepsilon=\left\{\varepsilon_x^0,\varepsilon_y^0,\gamma_{xy}^0\right\}^t,\quad k^b=\left\{k_x^b,k_y^b,k_{xy}^b\right\}^t,\quad k^s=\left\{k_x^s,k_y^s,k_{xy}^s\right\}^t, \tag{23b}$$

$$A=\begin{bmatrix} A_{11} & A_{12} & 0 \\ A_{12} & A_{22} & 0 \\ 0 & 0 & A_{66} \end{bmatrix},\quad D=\begin{bmatrix} D_{11} & D_{12} & 0 \\ D_{12} & D_{22} & 0 \\ 0 & 0 & D_{66} \end{bmatrix}, \tag{23c}$$

$$B^s=\begin{bmatrix} B_{11}^s & B_{12}^s & 0 \\ B_{12}^s & B_{22}^s & 0 \\ 0 & 0 & B_{66}^s \end{bmatrix},\quad D^s=\begin{bmatrix} D_{11}^s & D_{12}^s & 0 \\ D_{12}^s & D_{22}^s & 0 \\ 0 & 0 & D_{66}^s \end{bmatrix},\quad H^s=\begin{bmatrix} H_{11}^s & H_{12}^s & 0 \\ H_{12}^s & H_{22}^s & 0 \\ 0 & 0 & H_{66}^s \end{bmatrix}, \tag{23d}$$

$$S=\left\{S_{xz}^s,S_{yz}^s\right\}^t,\quad \gamma=\left\{\gamma_{xz},\gamma_{yz}\right\}^t,\quad A^s=\begin{bmatrix} A_{44}^s & 0 \\ 0 & A_{55}^s \end{bmatrix}, \tag{23e}$$

The stiffness coefficients A_{ij} and D_{ij}, etc., are defined as

$$\begin{Bmatrix} A_{11} & D_{11} & B_{11}^s & D_{11}^s & H_{11}^s \\ A_{12} & D_{12} & B_{12}^s & D_{12}^s & H_{12}^s \\ A_{66} & D_{66} & B_{66}^s & D_{66}^s & H_{66}^s \end{Bmatrix}=\int_{-\frac{h}{2}-C}^{\frac{h}{2}-C} Q_{11}\left(1,z_{ns}^2,f(z_{ns}),z_{ns}\,f(z_{ns}),f^2(z_{ns})\right)\begin{Bmatrix} 1 \\ \nu \\ \dfrac{1-\nu}{2} \end{Bmatrix}dz_{ns} \tag{24a}$$

and

$$\left(A_{22}, D_{22}, B_{22}^s, D_{22}^s, H_{22}^s\right) = \left(A_{11}, D_{11}, B_{11}^s, D_{11}^s, H_{11}^s\right) \tag{24b}$$

$$A_{44}^s = A_{55}^s = \int_{-\frac{h}{2}-C}^{\frac{h}{2}-C} \frac{E(z_{ns})}{2(1+\nu)}\left[g(z_{ns})\right]^2 dz_{ns}, \tag{24c}$$

By substituting Eq. (22) into Eq. (21), the equations of motion can be expressed in terms of displacements (δu_0, δv_0, δw_b, δw_s) as

$$A_{11}\frac{\partial^2 u_0}{\partial x^2} + A_{66}\frac{\partial^2 u_0}{\partial y^2} + \left(A_{12}+A_{66}\right)\frac{\partial^2 v_0}{\partial x \partial y} - \left(B_{12}^s + 2B_{66}^s\right)\frac{\partial^3 w_s}{\partial x \partial y^2} - B_{11}^s\frac{\partial^3 w_s}{\partial x^3} = I_0\ddot{u}_0 - I_1\frac{\partial \ddot{w}_b}{\partial x} - J_1\frac{\partial \ddot{w}_s}{\partial x}, \tag{25a}$$

$$A_{22}\frac{\partial^2 v_0}{\partial y^2} + A_{66}\frac{\partial^2 v_0}{\partial x^2} + \left(A_{12}+A_{66}\right)\frac{\partial^2 u_0}{\partial x \partial y} - \left(B_{12}^s + 2B_{66}^s\right)\frac{\partial^3 w_s}{\partial x^2 \partial y} - B_{22}^s\frac{\partial^3 w_s}{\partial y^3} = I_0\ddot{v}_0 - I_1\frac{\partial \ddot{w}_b}{\partial y} - J_1\frac{\partial \ddot{w}_s}{\partial y}, \tag{25b}$$

$$\begin{aligned} &- D_{11}\frac{\partial^4 w_b}{\partial x^4} - 2\left(D_{12}+2D_{66}\right)\frac{\partial^4 w_b}{\partial x^2 \partial y^2} - D_{22}\frac{\partial^4 w_b}{\partial y^4} \\ &- D_{11}^s\frac{\partial^4 w_s}{\partial x^4} - 2\left(D_{12}^s + 2D_{66}^s\right)\frac{\partial^4 w_s}{\partial x^2 \partial y^2} - D_{22}^s\frac{\partial^4 w_s}{\partial y^4} + q \\ &= I_0\left(\ddot{w}_b + \ddot{w}_s\right) + I_1\left(\frac{\partial \ddot{u}_0}{\partial x} + \frac{\partial \ddot{v}_0}{\partial y}\right) - I_2\nabla^2\ddot{w}_b - J_2\nabla^2\ddot{w}_s, \end{aligned} \tag{25c}$$

$$\begin{aligned} &B_{11}^s\frac{\partial^3 u_0}{\partial x^3} + \left(B_{12}^s + 2B_{66}^s\right)\frac{\partial^3 u_0}{\partial x \partial y^2} + \left(B_{12}^s + 2B_{66}^s\right)\frac{\partial^3 v_0}{\partial x^2 \partial y} + B_{22}^s\frac{\partial^3 v_0}{\partial y^3} - D_{11}^s\frac{\partial^4 w_b}{\partial x^4} \\ &- 2\left(D_{12}^s + 2D_{66}^s\right)\frac{\partial^4 w_b}{\partial x^2 \partial y^2} - D_{22}^s\frac{\partial^4 w_b}{\partial y^4} - H_{11}^s\frac{\partial^4 w_s}{\partial x^4} \\ &- 2\left(H_{12}^s + 2H_{66}^s\right)\frac{\partial^4 w_s}{\partial x^2 \partial y^2} - H_{22}^s\frac{\partial^4 w_s}{\partial y^4} + A_{55}^s\frac{\partial^2 w_s}{\partial x^2} \\ &+ A_{44}^s\frac{\partial^2 w_s}{\partial y^2} + q = I_0\left(\ddot{w}_b + \ddot{w}_s\right) + J_1\left(\frac{\partial \ddot{u}_0}{\partial x} + \frac{\partial \ddot{v}_0}{\partial y}\right) - J_2\nabla^2\ddot{w}_b - K_2\nabla^2\ddot{w}_s \end{aligned} \tag{25d}$$

3. Closed-form solution for simply supported plates

Rectangular plates are generally classified according to the type of support used. Here, we are concerned with the exact solutions of Eqs. (25) for a simply supported FG plate. Based on the Navier approach, the solutions are assumed as

$$\begin{Bmatrix} u_0 \\ v_0 \\ w_b \\ w_s \end{Bmatrix} = \sum_{m=1}^{\infty}\sum_{n=1}^{\infty} \begin{Bmatrix} U_{mn} e^{i\omega t} \cos(\lambda x)\sin(\mu y) \\ V_{mn} e^{i\omega t} \sin(\lambda x)\cos(\mu y) \\ W_{bmn} e^{i\omega t} \sin(\lambda x)\sin(\mu y) \\ W_{smn} e^{i\omega t} \sin(\lambda x)\sin(\mu y) \end{Bmatrix} \tag{26}$$

where U_{mn}, V_{mn}, W_{bmn} and W_{smn} are arbitrary parameters to be determined, ω is the eigenfrequency associated with (m, n)th eigenmode, and $\lambda = m\pi / a$ and $\mu = n\pi / b$.

The transverse load q is also expanded in the double-Fourier sine series as

$$q(x,y) = \sum_{m=1}^{\infty}\sum_{n=1}^{\infty} q_{mn} \sin(\lambda x)\sin(\mu y) \tag{27}$$

For the case of a sinusoidally distributed load, we have

$$m = n = 1 \quad \text{and} \quad q_{11} = q_0 \tag{28}$$

where q_0 represents the intensity of the load at the plate centre.

Substituting Eqs. (26) and (27) into Eq. (25), the analytical solutions can be obtained from

$$\left(\begin{bmatrix} a_{11} & a_{12} & 0 & a_{14} \\ a_{12} & a_{22} & 0 & a_{24} \\ 0 & 0 & a_{33} & a_{34} \\ a_{14} & a_{24} & a_{34} & a_{44} \end{bmatrix} - \omega^2 \begin{bmatrix} m_{11} & 0 & m_{13} & m_{14} \\ 0 & m_{22} & m_{23} & m_{24} \\ m_{13} & m_{23} & m_{33} & m_{34} \\ m_{14} & m_{24} & m_{34} & m_{44} \end{bmatrix} \right) \begin{Bmatrix} U_{mn} \\ V_{mn} \\ W_{bmn} \\ W_{smn} \end{Bmatrix} = \begin{Bmatrix} 0 \\ 0 \\ q_{mn} \\ q_{mn} \end{Bmatrix} \tag{29}$$

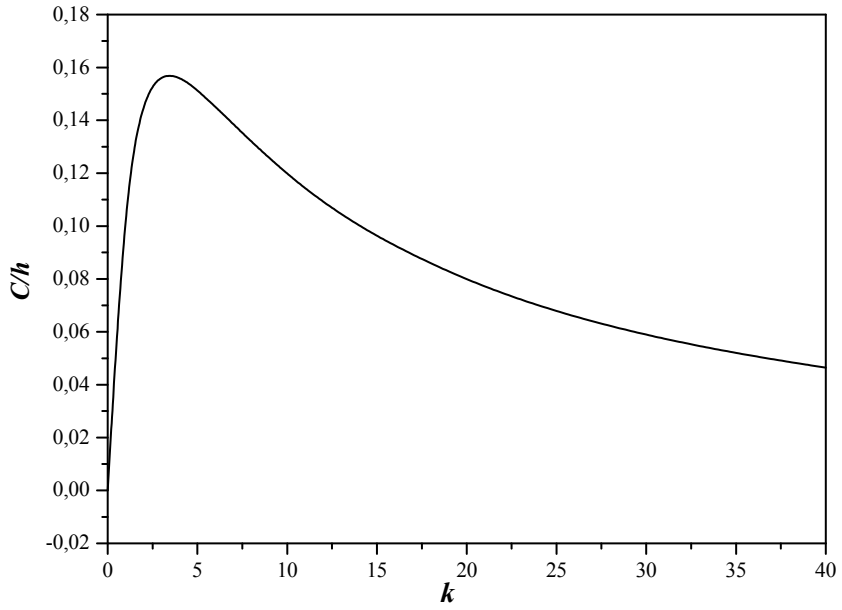

Fig. 2 Variation of the neutral surface position versus the material parameter k

Table 1 Material properties used in the FG plate

Properties	Metal aluminum (Al)	Ceramic	
		Alumina (Al_2O_3)	Zirconia (ZrO_2)
$\boldsymbol{E}$ (GPa)	70	380	200
$\boldsymbol{\rho}$ (kg/m^3)	2702	3800	5700

in which

$$
\begin{aligned}
a_{11} &= A_{11}\lambda^2 + A_{66}\mu^2 \\
a_{12} &= \lambda\,\mu\left(A_{12} + A_{66}\right) \\
a_{14} &= -\lambda\left[B_{11}^s\lambda^2 + (B_{12}^s + 2B_{66}^s)\,\mu^2\right] \\
a_{22} &= A_{66}\lambda^2 + A_{22}\mu^2 \\
a_{24} &= -\mu\left[(B_{12}^s + 2B_{66}^s)\,\lambda^2 + B_{22}^s\mu^2\right] \\
a_{33} &= D_{11}\lambda^4 + 2(D_{12} + 2D_{66})\lambda^2\mu^2 + D_{22}\mu^4 \\
a_{34} &= D_{11}^s\lambda^4 + 2(D_{12}^s + 2D_{66}^s)\lambda^2\,\mu^2 + D_{22}^s\,\mu^4 \\
a_{44} &= H_{11}^s\lambda^4 + 2(H_{11}^s + 2H_{66}^s)\lambda^2\mu^2 + H_{22}^s\mu^4 - A_{55}^s\lambda^2 - A_{44}^s\mu^2 \\
m_{11} &= m_{22} = -I_0, \quad m_{13} = \lambda I_1, \quad m_{14} = \lambda J_1, \quad m_{23} = \mu I_1 \\
m_{24} &= \mu J_1, \quad m_{33} = -\left(I_0 + I_2\left(\lambda^2 + \mu^2\right)\right) \\
m_{34} &= -\left(I_0 + J_2\left(\lambda^2 + \mu^2\right)\right), \quad m_{44} = -\left(I_0 + K_2\left(\lambda^2 + \mu^2\right)\right),
\end{aligned}
\tag{30}
$$

4. Numerical results

In this section, various numerical examples are presented and discussed to verify the accuracy of the present theory in predicting the bending and free vibration responses of simply supported FG plates. Two types of FG plates of Al/Al_2O_3 and Al/ZrO_2 are used in this study, in which their material properties are listed in Table 1. For all calculations, the Poisson's ratio is taken as 0.3

Fig. 2 presents the variation of non-dimensional parameter C/h versus the material parameter k of Al/Al_2O_3 functionally graded plate. It can be observed when the material parameter of FGM becomes zero (fully ceramic) or infinity (fully metallic); the neutral surface coincides on the middle surface, as expected.

4.1 Bending analysis

For bending analysis, a plate subjected to a sinusoidal load is considered. For convenience, the following dimensionless forms are used

$$
\bar{z}_{ms} = \frac{z_{ms}}{h}, \qquad \bar{w} = \frac{10h^3E_c}{a^4q_0}w\left(\frac{a}{2},\frac{b}{2},\bar{z}_{ms}\right), \quad \bar{\sigma}_x = \frac{h}{aq_0}\sigma_x\left(\frac{a}{2},\frac{b}{2},\bar{z}_{ms}\right),
$$

$$
\bar{\tau}_{xy} = \frac{h}{aq_0}\tau_{xy}\left(0,0,\bar{z}_{ms}\right), \quad \bar{\tau}_{xz} = \frac{h}{aq_0}\tau_{xz}\left(0,\frac{b}{2},\bar{z}_{ms}\right), \qquad \bar{\sigma}_z = \sigma_z\left(\frac{a}{2},\frac{b}{2},\bar{z}_{ms}\right)
$$

Table 2 Dimensionless stresses and displacements of a functionally graded square plate (a / h = 10)

k	Method	$\bar{w}$	$\bar{\sigma}_x$	$\bar{\sigma}_y$	$\bar{\tau}_{xy}$	$\bar{\tau}_{xz}$	$\bar{\tau}_{yz}$
	Zenkour (2006)	0.2960	1.9955	1.3121	0.7065	0.2462	0.2132
	Present n = 3	0.2960	1.9943	1.3123	0.7066	0.2385	0.2120
Ceramic	Present n = 5	0.2957	1.9894	1.3134	0.7072	0.2045	0.2020
	Present n = 7	0.2953	1.9864	1.3145	0.7078	0.1915	0.1912
	Present n = 9	0.2950	1.9844	1.3153	0.7082	0.1844	0.1844
	Zenkour (2006)	0.5889	3.0870	1.4894	0.6110	0.2462	0.2622
	Present n = 3	0.5889	3.0850	1.4898	0.6111	0.2385	0.2607
1	Present n = 5	0.5884	3.0767	1.4914	0.6114	0.2045	0.2484
	Present n = 7	0.5877	3.0716	1.4930	0.6117	0.1915	0.2352
	Present n = 9	0.5872	3.0683	1.4941	0.6119	0.1844	0.2267
	Zenkour (2006)	0.8819	4.0693	1.1783	0.5667	0.2029	0.2580
	Present n = 3	0.8814	4.0655	1.1793	0.5669	0.1943	0.2536
4	Present n = 5	0.8784	4.0501	1.1834	0.5677	0.1586	0.2301
	Present n = 7	0.8760	4.0411	1.1862	0.5682	0.1444	0.2117
	Present n = 9	0.8744	4.0353	1.1880	0.5685	0.1365	1.1880
	Zenkour (2006)	1.0089	5.0890	0.8775	0.5894	0.2198	0.2041
	Present n = 3	1.0087	5.0848	0.8784	0.5895	0.2113	0.2014
10	Present n = 5	1.0055	5.0678	0.8824	0.5904	0.1747	0.1850
	Present n = 7	1.0024	5.0570	0.8851	0.5911	0.1593	0.17063
	Present n = 9	1.0000	5.0499	0.8868	0.5915	0.1504	0.1612
	Zenkour (2006)	1.6070	1.9955	1.3121	0.7065	0.2462	0.2132
	Present n = 3	1.6071	1.9943	1.3123	0.7066	0.2385	0.2120
Metal	Present n = 5	1.6054	1.9894	1.3134	0.7072	0.2045	0.2020
	Present n = 7	1.6033	1.9864	1.3145	0.7078	0.1915	0.1912
	Present n = 9	1.6017	1.9844	1.3153	0.7082	0.1844	0.1844

Table 2 contains nondimensional stresses and displacements of a simply supported FG square plate of a / h = 10. It can be found that the present n-order four variable refined theory produces the close results to those of Zenkour (2006).

The nondimensional transverse normal displacement and transverse shear stress are compared in Table 3 with those obtained by Matsunaga (2009). Varying the number of power law index and the side to thickness ratio, the results are in good agreement with those of Matsunaga (2009).

It should be noted that the present theory contains four unknowns as against five or more in the case of other higher order theories. It can be concluded that the present theory is not only accurate but also efficient in predicting the responses of FG plates.

Table 3 Comparison of the dimensionless deflections and transverse shear stresses in a square FG-plate subjected to sinusoidally distributed load

k	Method	$a/h = 5$		$a/h = 10$	
		$wE_c / q_0 h$	$\tau_{xz}(0, b/2)/q_0$	$wE_c / q_0 h$	$\tau_{xz}(0, b/2)/q_0$
0	Matsunaga (2009)	0.2098	01186	0.2943	0.2383
	Present $n = 3$	0.2145	0.1190	0.2960	0.2385
	Present $n = 5$	0.2138	0.1022	0.2957	0.2045
	Present $n = 7$	0.2128	0.0957	0.2953	0.1915
	Present $n = 9$	0.2121	0.0922	0.2950	0.1844
0.5	Matsunaga (2009)	0.3179	0.1209	0.4504	0.2431
	Present $n = 3$	0.3235	0.1217	0.4537	0.2439
	Present $n = 5$	0.3225	0.1049	0.4533	0.2100
	Present $n = 7$	0.3213	0.0985	0.4528	0.1971
	Present $n = 9$	0.3204	0.0951	0.4524	0.1902
1	Matsunaga (2009)	0.4139	0.1184	0.5875	0.2383
	Present $n = 3$	0.4179	0.1190	0.5889	0.2385
	Present $n = 5$	0.4167	0.1022	0.5884	0.2045
	Present $n = 7$	0.4151	0.0957	0.5877	0.1915
	Present $n = 9$	0.4139	0.0922	0.5872	0.1844
4	Matsunaga (2009)	0.6511	0.1076	0.8823	0.2175
	Present $n = 3$	0.6505	0.0969	0.8815	0.1944
	Present $n = 5$	0.6431	0.0792	0.8784	0.1586
	Present $n = 7$	0.6373	0.0721	0.8760	0.1444
	Present $n = 9$	0.6332	0.0682	0.8744	0.1365
10	Matsunaga (2009)	0.7624	0.1078	0.1007	0.2167
	Present $n = 3$	0.7672	0.1053	1.0087	0.2113
	Present $n = 5$	0.7596	0.0873	1.0055	0.1747
	Present $n = 7$	0.7520	0.0796	1.0024	0.1593
	Present $n = 9$	0.7461	0.0752	1.0000	0.1504

In Figs. 3 and 4, the variation of the center deflection with the aspect and side-to-thickness ratios is presented, respectively. The deflection is maximum for the metallic plate and minimum for the ceramic plate. The difference increases as the aspect ratio increases while it may be unchanged with the increase of side-to-thickness ratio. One of the main inferences from the analysis is that the response of FGM plates is intermediate to that of the ceramic and metal homogeneous plates.

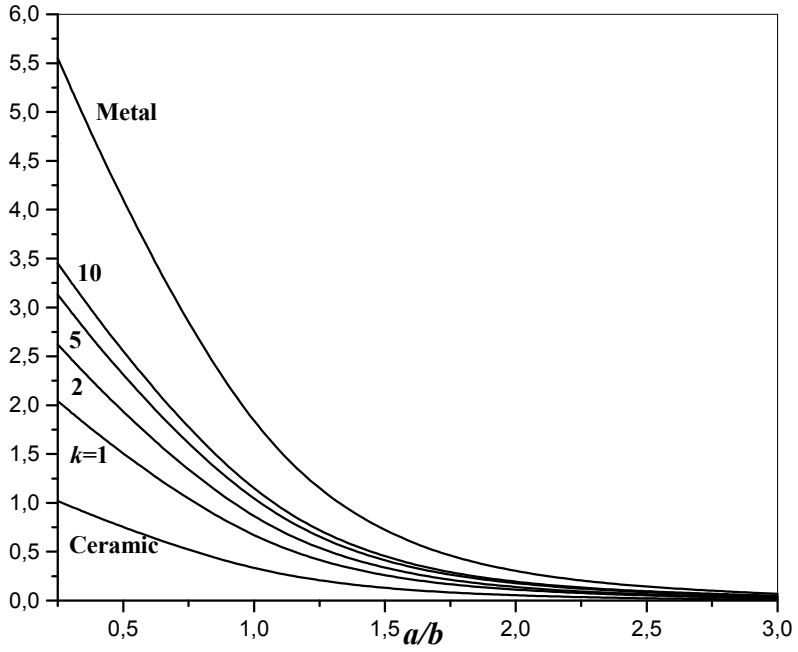

Fig. 3 Dimensionless center deflection $\bar{w}$ as function of the aspect (a / b) of an FG plate (a / h = 10, n = 3)

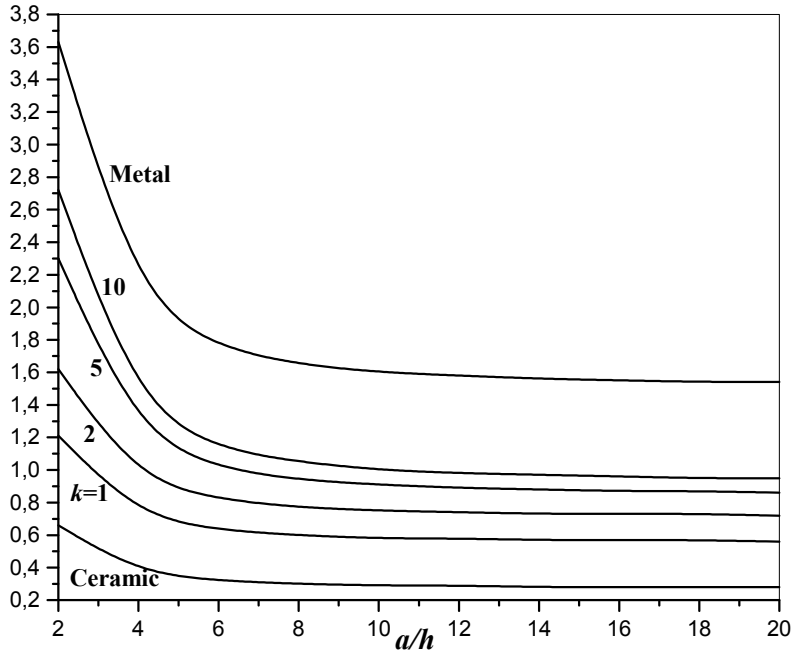

Fig. 4 Dimensionless center deflection $\bar{w}$ as function of the side-to-thickness ratio (a / h) of an FG square plate (n = 3)

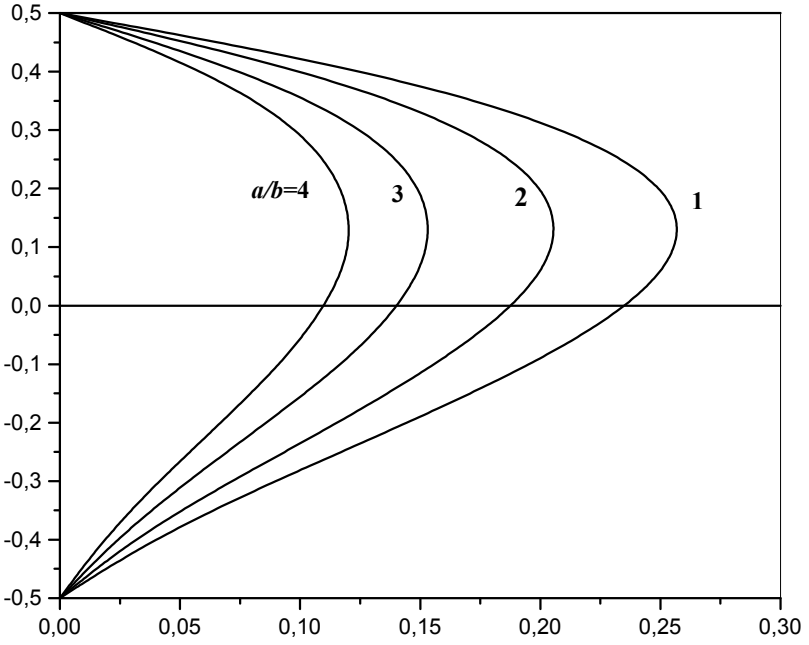

Fig. 5 Variation of transversal shear stress ($\bar{\tau}_{xz}$) through-the-thickness of an FG plate for different values of the aspect ratio (a / h = 10, k = 1, n = 3)

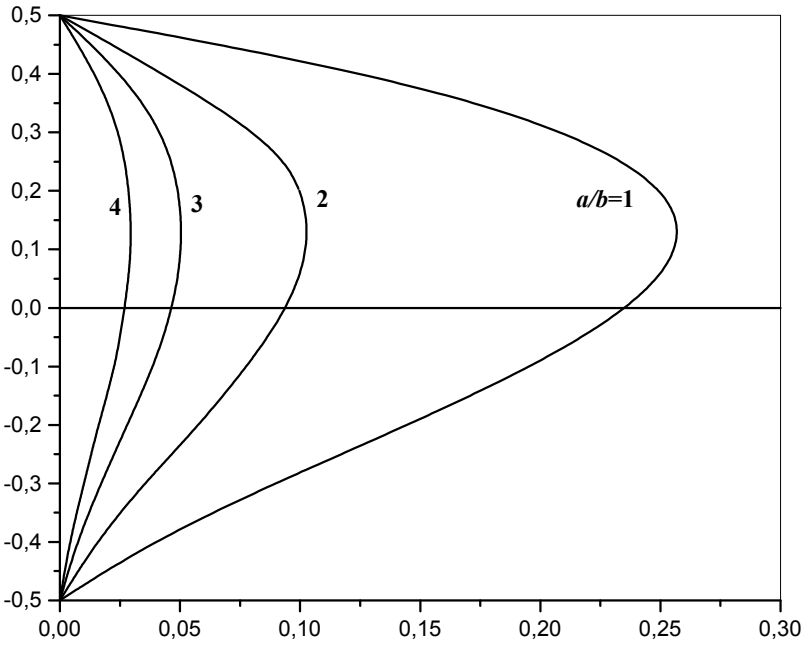

Fig. 6 Variation of transversal shear stress ($\bar{\tau}_{xz}$) through-the-thickness of an FG plate for different values of the aspect ratio (a / h = 10, k = 1, n = 3)

Figs. 5-9 present the through-the-thickness distributions of the shear stresses $\bar{\tau}_{yz}$ and $\bar{\tau}_{xz}$; the normal stresses $\bar{\sigma}_x$ and $\bar{\sigma}_y$, and the longitudinal tangential stress $\bar{\tau}_{xy}$ in the FG plate under the sinusoidal load. The volume fraction exponent of the FG plate is taken as $k = 1$ in these figures. The through-the-thickness distributions of the shear stresses $\bar{\tau}_{yz}$ and $\bar{\tau}_{xz}$ are not parabolic and the stresses increase as the aspect ratio decreases (Figs. 5 and 6). It is to be noted that the maximum value occurs at $\bar{z} \cong 0.135$ and not at the plate center as in the homogeneous case.

As indicated in Figs. 7 and 8, the normal stresses, $\bar{\sigma}_x$ and $\bar{\sigma}_y$, are compressive throughout the plate up to $z = C$ ($\bar{z} \cong 0.115$) the distance of neutral surface from the middle surface and then they become tensile. The maximum compressive stresses occur at a point on the bottom surface and the maximum tensile stresses occur, of course, at a point on the top surface of the FG plate. However, the tensile and compressive values of the longitudinal tangential stress, $\bar{\tau}_{xy}$ (Fig. 9), are maximum at a point on the bottom and top surfaces of the FG plate, respectively. It is clear that the minimum value of zero for all in-plane stresses $\bar{\sigma}_x$; $\bar{\sigma}_y$ and $\bar{\tau}_{xy}$ occurs at $z = C$ and this irrespective of the aspect and side-to-thickness ratios.

The effect of material anisotropy on the maximum deflections of simply supported FG square plate ($a / h = 10$) is presented in Fig. 10. It is clear that the deflections decrease smoothly as the volume fraction exponent decreases and as the ratio of metal-to-ceramic moduli increases.

4.2 Free vibration analysis

In this section, various numerical examples are presented and discussed to verify the accuracy

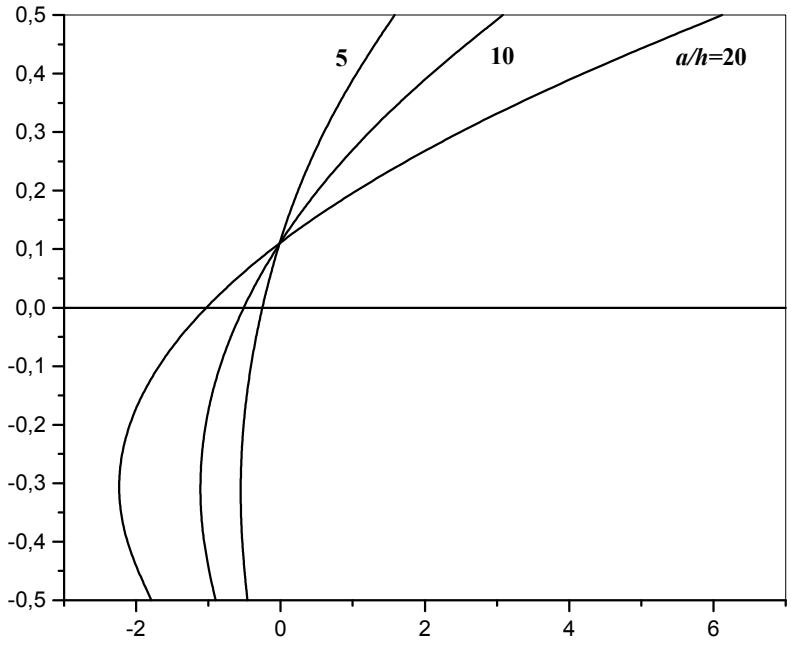

Fig. 7 Variation of normal stress ($\bar{\sigma}_x$) through-the-thickness of an FG square plate for different values of the side-to-thickness ratio ($\boldsymbol{k} = 1$, $\boldsymbol{n} = 3$)

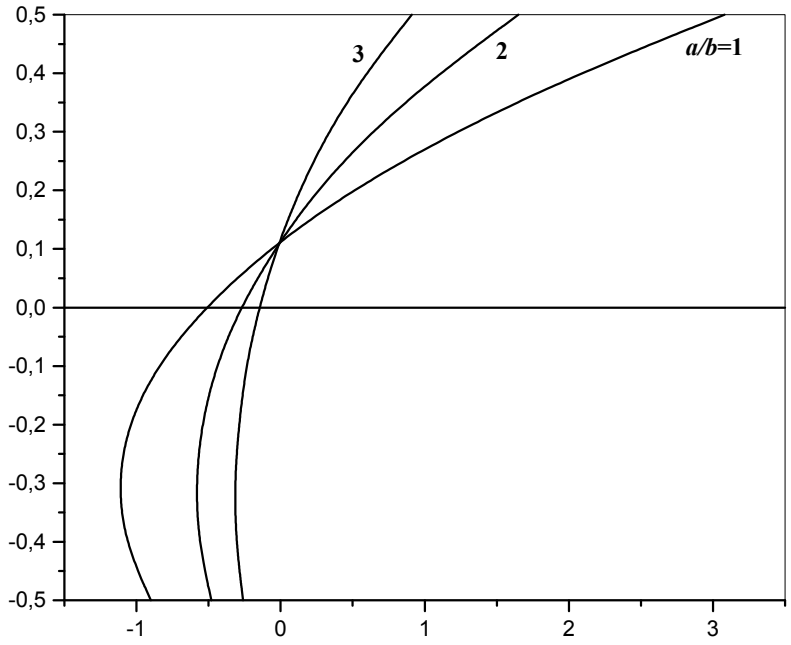

Fig. 8 Variation of normal stress ($\bar{\sigma}_y$) through-the-thickness of an FG plate for different values of the aspect ratio (***a*** / ***h*** = 10, ***k*** = 1, ***n*** = 3)

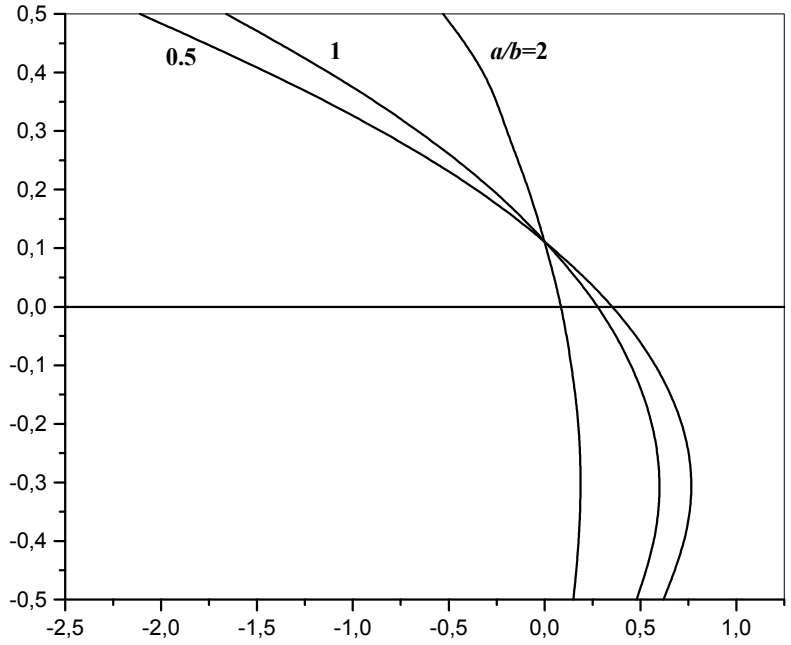

Fig. 9 Variation of tangential stress ($\bar{\tau}_{xy}$) through-the-thickness of an FG plate for different values of the aspect ratio (***a*** / ***h*** = 10, ***k*** = 1, ***n*** = 3)

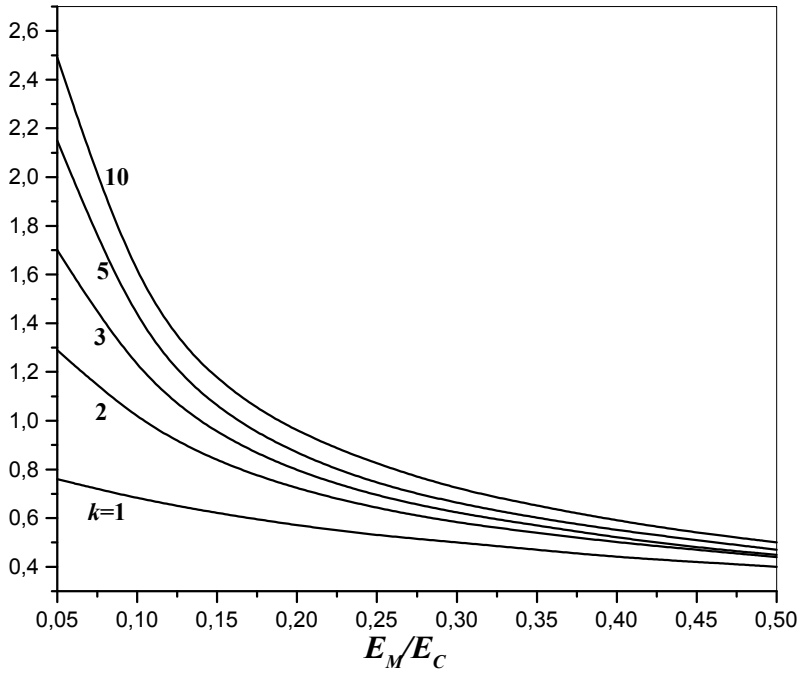

Fig. 10 The effect of material anisotropy on the dimensionless maximum deflection ($\bar{w}$) of an FG plate for different values of k (a / h = 10, n = 3)

of the present theory in predicting the natural frequency of simply supported plates. For convenience, following natural frequency parameter is used in presenting the numerical results in tabular and graphical forms

$$\bar{\beta} = \omega h\sqrt{\rho_m / E_m}, \quad \hat{\beta} = \omega h\sqrt{\rho_c / E_c}, \quad \bar{\omega} = \frac{\omega a^2}{h}\sqrt{\rho_c / E_c},$$

The first verification is performed for Al/ZrO_2 square plates with different values of thickness ratio a / h and power law index k. The fundamental frequency parameters $\bar{\beta}$ obtained using the present theory are compared with those of 3-D exact solutions of Vel and Batra (2004), 2-D higher-order theory solutions of Matsunaga (2008), and Reddy's theory with analytical method solutions of Hosseini-Hashemi *et al*. (2011a) in Table 4. It can be seen that for the plate with k = 0, that is, fully ceramic isotropic plate, the results of present theory are well in agreement with those of other solutions (Matsunaga 2008, Vel and Batra 2004, Hosseini-Hashemi *et al*. 2011a). However, for FG plate with non-zero values of k, the results of present n-order four variable refined theory and other shear deformation theories are higher than those obtained by 3-D exact solutions of Vel and Batra (2004).

The fundamental frequency and the lowest third frequency parameters $\hat{\beta}$ are presented in Table 5 for a square Al/Al_2O_3 plate with thickness ratio varied from 5 to 20 and power law index varied from 0 to 10. It can be seen that the results obtained by the present n-order four variable refined theory are in good agreement with those reported by Hosseini-Hashemi *et al*. (2011a) based on

Reddy's theory.

The lowest four frequency parameters $\bar{\omega}$ obtained from present *n*-order four variable refined theory are compared with those reported by Hosseini-Hashemi et al. (2011b) based on first shear deformation theory (FSDT) in Table 6 for rectangular Al/Al_2O_3 plate ($b = 2a$) with thickness ratio varied from 5 to 20 and power law index varied from 0 to 10. It can be observed that the FSDT (Hosseini-Hashemi *et al*. 2011b) gives accurate results for moderately thick plate at lower modes of vibration.

Table 4 Comparison of fundamental frequency parameter $\bar{\beta}$ of Al/ZrO_2 square plate

Method	$k = 0$		$k = 1$			a/h		
	$a/h = \sqrt{10}$	$a/h = 10$	$a/h = 5$	$a/h = 10$	$a/h = 20$	$k = 2$	$k = 3$	$k = 5$
3D (Vel and Batra 2004)	0.4658	0.0578	0.2192	0.0596	0.0153	0.2197	0.2211	0.2225
Matsunaga (2008)	0.4658	0.0578	0.2285	0.0619	0.0158	0.2264	0.2270	0.2281
Hosseini-Hashemi *et al*. (2011a)	0.4623	0.0577	0.2276	0.0619	0.0158	0.2256	0.2263	0.2272
Present $n = 3$	0.4622	0.0576	0.2276	0.0618	0.0158	0.2256	0.2262	0.2271
Present $n = 5$	0.4634	0.0577	0.2280	0.0618	0.0158	0.2262	0.2269	0.2280
Present $n = 7$	0.4651	0.0577	0.2284	0.0619	0.0158	0.2267	0.2276	0.2287
Present $n = 9$	0.4665	0.0577	0.2287	0.0619	0.0158	0.2271	0.2281	0.2293

Table 5 Comparison of natural frequency parameter $\hat{\beta}$ of AL/Al_2O_3 square plate

a/h	Mode no. (m, n)	Method	k				
			0	0.5	1	4	10
5	(1,1)	Hosseini-Hashemi *et al*. (2011a)	0.2113	0.1807	0.1631	0.1378	0.1301
		Present $n = 3$	0.2112	0.1807	0.1631	0.1378	0.1300
		Present $n = 5$	0.2115	0.1809	0.1633	0.1385	0.1306
		Present $n = 7$	0.2120	0.1812	0.1636	0.1390	0.1312
		Present $n = 9$	0.2123	0.1815	0.1638	0.1394	0.1316
5	(1,2)	Hosseini-Hashemi *et al*. (2011a)	0.4623	0.3989	0.3607	0.2980	0.7271
		Present $n = 3$	0.4622	0.3988	0.3606	0.2979	0.2770
		Present $n = 5$	0.4634	0.3997	0.3614	0.3004	0.2790
		Present $n = 7$	0.4651	0.4010	0.3626	0.3026	0.2812
		Present $n = 9$	0.4665	0.4020	0.3635	0.3042	0.2830

Table 5 Continued

a/h	Mode no. (m, n)	Method	k				
			0	0.5	1	4	10
5	(2,2)	Hosseini-Hashemi *et al*. (2011a)	0.6688	0.5803	0.5254	0.4284	0.3948
		Present $n = 3$	0.6688	0.5802	0.5254	0.4283	0.3948
		Present $n = 5$	0.6707	0.5817	0.5267	0.4326	0.3980
		Present $n = 7$	0.6739	0.5842	0.5288	0.4365	0.4019
		Present $n = 9$	0.6764	0.5860	0.5305	0.4393	0.4050
10	(1,1)	Hosseini-Hashemi *et al*. (2011a)	0.0577	0.0490	0.0442	0.0381	0.0364
		Present $n = 3$	0.0576	0.0490	0.0441	0.0380	0.0363
		Present $n = 5$	0.0577	0.0490	0.0442	0.0381	0.0364
		Present $n = 7$	0.0577	0.0490	0.0442	0.0381	0.0364
		Present $n = 9$	0.0577	0.0491	0.0442	0.0382	0.0365
	(1,2)	Hosseini-Hashemi *et al*. (2011a)	0.1377	0.1174	0.1059	0.0903	0.0856
		Present $n = 3$	0.1376	0.1173	0.1059	0.0902	0.0856
		Present $n = 5$	0.1378	0.1174	0.1060	0.0905	0.0859
		Present $n = 7$	0.1379	0.1176	0.1061	0.0908	0.0861
		Present $n = 9$	0.1381	0.1177	0.1062	0.0910	0.0863
	(2,2)	Hosseini-Hashemi *et al*. (2011a)	0.2113	0.1807	0.1631	0.1378	0.1301
		Present $n = 3$	0.2112	0.1807	0.1631	0.1378	0.1300
		Present $n = 5$	0.2115	0.1809	0.1633	0.1385	0.1306
		Present $n = 7$	0.2120	0.1812	0.1636	0.1390	0.1312
		Present $n = 9$	0.2123	0.1815	0.1638	0.1394	0.1316
20	(1,1)	Hosseini-Hashemi *et al*. (2011a)	0.0148	0.0125	0.0113	0.0098	0.0094
		Present $n = 3$	0.0147	0.0125	0.0113	0.0098	0.0094
		Present $n = 5$	0.0148	0.0125	0.0113	0.0098	0.0094
		Present $n = 7$	0.0148	0.0125	0.0113	0.0098	0.0094
		Present $n = 9$	0.0148	0.0125	0.0113	0.0098	0.0094

Table 6 Comparison of frequency parameter $\bar{\omega}$ of AL/Al_2O_3 rectangular plate ($\boldsymbol{b} = 2\boldsymbol{a}$)

$\boldsymbol{a}$ / $\boldsymbol{h}$	Mode no. (m, n)	Method	$\boldsymbol{k}$						
			0	0.5	1	2	5	8	10
5	1 (1,1)	Hosseini-Hashemi *et al*. (2011b)	3.4409	2.9322	2.6473	2.4017	2.2528	2.1985	2.1677
		Present $\boldsymbol{n} = 3$	3.4412	2.9346	2.6475	2.3948	2.2271	2.1696	2.1406
		Present $\boldsymbol{n} = 5$	3.4451	2.9374	2.6500	2.3987	2.2363	2.1781	2.1475
		Present $\boldsymbol{n} = 7$	3.4499	2.9409	2.6532	2.4026	2.2435	2.1856	2.1545
		Present $\boldsymbol{n} = 9$	3.4536	2.9436	2.6556	2.4055	2.2486	2.1912	2.1598
	2 (1,2)	Hosseini-Hashemi *et al*. (2011b)	5.2802	4.5122	4.0773	3.6953	3.4492	3.3587	3.3094
		Present $\boldsymbol{n} = 3$	5.2813	4.5179	4.0780	3.6805	3.3938	3.2964	3.2513
		Present $\boldsymbol{n} = 5$	5.2896	4.5240	4.0836	3.6889	3.4134	3.3143	3.2807
		Present $\boldsymbol{n} = 7$	5.3003	4.5318	4.0906	3.6975	3.4290	3.3305	3.2807
		Present $\boldsymbol{n} = 9$	5.3087	4.5379	4.0961	3.7041	3.4402	3.3427	3.2923
	3 (1,3)	Hosseini-Hashemi *et al*. (2011b)	8.0710	6.9231	6.2636	5.6695	5.2579	5.1045	5.0253
		Present $\boldsymbol{n} = 3$	8.0748	6.9366	6.2662	5.6389	5.1424	4.9757	4.9055
		Present $\boldsymbol{n} = 5$	8.0920	6.9493	6.2777	5.6562	5.1825	5.0119	4.9345
		Present $\boldsymbol{n} = 7$	8.1150	6.9662	6.2930	5.6748	5.2154	5.0456	4.9653
		Present $\boldsymbol{n} = 9$	8.1331	6.9795	6.3050	5.6889	5.2390	5.0710	4.9896
	4 (2,1)	Hosseini-Hashemi *et al*. (2011b)	9.7416	8.6926	7.8711	7.1189	6.5749	5.9062	5.7518
		Present $\boldsymbol{n} = 3$	10.1163	8.7138	7.8761	7.0750	6.4073	6.1846	6.0954
		Present $\boldsymbol{n} = 5$	10.1409	8.7322	7.8926	7.0998	6.4648	6.2360	6.1363
		Present $\boldsymbol{n} = 7$	10.1749	8.7575	7.9154	7.1272	6.5127	6.2848	6.1810
		Present $\boldsymbol{n} = 9$	10.2018	8.7773	7.9335	7.1483	6.5474	6.3219	6.2163
10	1 (1,1)	Hosseini-Hashemi *et al*. (2011b)	3.6518	3.0983	2.7937	2.5386	2.3998	2.3504	2.3197
		Present $\boldsymbol{n} = 3$	3.6517	3.0990	2.7936	2.5364	2.3916	2.3410	2.3110
		Present $\boldsymbol{n} = 5$	3.6530	3.0998	2.7944	2.5376	2.3945	2.3438	2.3132
		Present $\boldsymbol{n} = 7$	3.6544	3.1009	2.7954	2.5388	2.3968	2.3462	2.3155
		Present $\boldsymbol{n} = 9$	3.6556	3.1017	2.7961	2.5397	2.3984	2.3480	2.3172
	2 (1,2)	Hosseini-Hashemi *et al*. (2011b)	5.7693	4.8997	4.4192	4.0142	3.7881	3.7072	3.6580
		Present $\boldsymbol{n} = 3$	5.7694	4.9014	4.4192	4.0089	3.7682	3.6845	3.6368
		Present $\boldsymbol{n} = 5$	5.7724	4.9035	4.4211	4.0119	3.7754	3.6913	3.6423
		Present $\boldsymbol{n} = 7$	5.7760	4.9061	4.4235	4.0148	3.7809	3.6971	3.6477
		Present $\boldsymbol{n} = 9$	5.7788	4.9081	4.4253	4.0170	3.7849	3.7014	3.6519

Table 6 Continued

a/h	Mode no. (m, n)	Method	k						
			0	0.5	1	2	5	8	10
10	3 (1,3)	Hosseini-Hashemi *et al*. (2011b)	9.1876	7.8145	7.0512	6.4015	6.0247	5.8887	5.8086
		Present $n = 3$	9.1880	7.8189	7.0514	6.3886	5.9764	5.8340	5.7574
		Present $n = 5$	9.1953	7.8241	7.0562	6.3959	5.9938	5.8502	5.7706
		Present $n = 7$	9.2042	7.8304	7.0620	6.4031	6.0073	5.8644	5.7837
		Present $n = 9$	9.2111	7.8354	7.0665	6.4086	6.0169	5.8749	5.7938
	4 (2,1)	Hosseini-Hashemi *et al*. (2011b)	11.8310	10.0740	9.0928	8.2515	7.7505	7.5688	7.4639
		Present $n = 3$	11.8314	10.0809	9.0933	8.2308	7.6731	7.4812	7.3821
		Present $n = 5$	11.8431	10.0893	9.1009	8.2425	7.7009	7.5070	7.4030
		Present $n = 7$	11.8576	10.0997	9.1104	8.2543	7.7226	7.5298	7.4240
		Present $n = 9$	11.8688	10.1078	9.1177	8.2631	7.7381	7.5466	7.4402

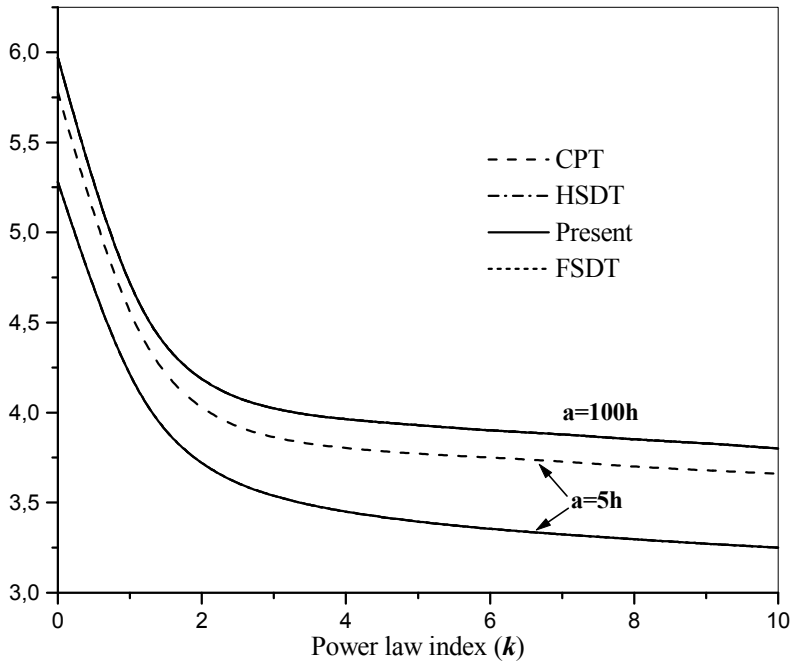

Fig. 11 The effect of power law index on fundamental frequency parameter ($\bar{\omega}$) of square FG plate ($n = 3$)

Fig. 11 illustrates the variation of fundamental frequency parameters of square plate with respect to power law index, k. The thickness ratios a/h are assumed to be 5 (corresponding to thick plate) and 100 (corresponding to thin plate). It can be seen that the fundamental frequency

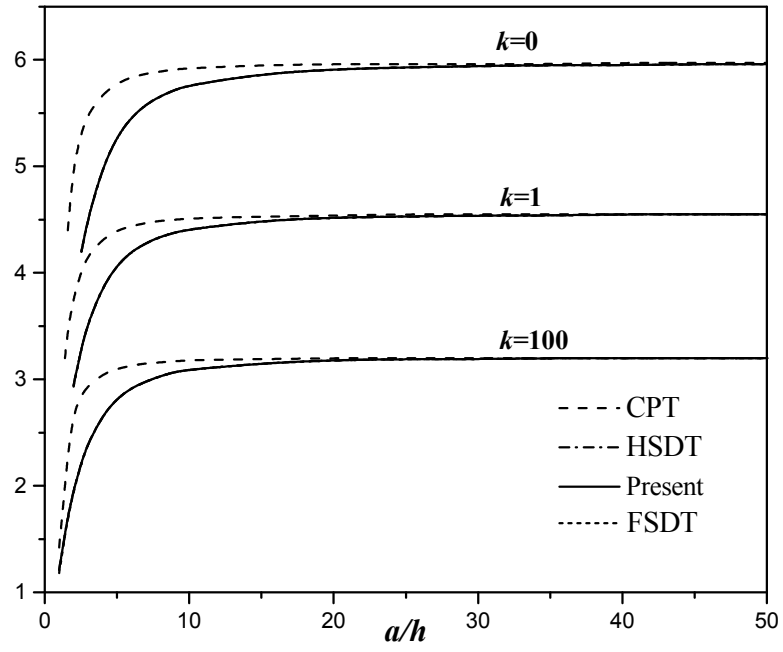

Fig. 12 The effect of thickness ratio on fundamental frequency parameter ($\bar{\omega}$) of square FG plate ($n = 3$)

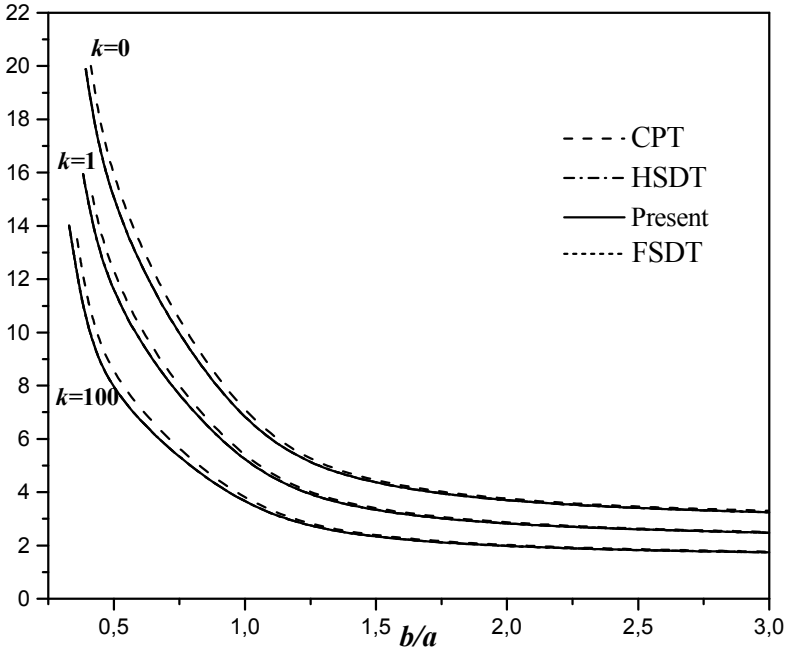

Fig. 13 The effect of aspect ratio on fundamental frequency parameter ($\bar{\omega}$) of FG plate ($a = 10h$, $n = 3$)

parameter decreases as the power law index increases. This is due to the fact that increasing the power law index increases the volume fraction of metal. Also, the frequency parameters of fully ceramic plates are considerably higher than those of FG plates. Furthermore, the results predicted by the present theory, the higher order shear deformation theory (HSDT) based on Reddy's theory and FSDT are identical, and the classical plate theory (CPT) overestimates frequency parameter of FG plates. The difference between CPT and present theory is considerable for thick plate, but it can be neglected for thin plates.

The variation of fundamental frequency parameter of square plate versus thickness ratio a/h is shown in Fig. 12. It is observed that the fundamental frequency parameter increases by the increase in thickness ratio, and the variation of fundamental frequency parameter is remarkable when the thickness ratio is smaller than 5. Also, the CPT overestimates the frequency parameter of FG plates, and the discrepancy between the CPT and present curves is negligible when the thickness ratio is greater than 10. The effect of aspect ratio b/a on the frequency parameter of plate ($a/h = 10$) is presented in Fig. 13. It can be found that that the frequency parameter decreases by the increase in the aspect ratio.

5. Conclusions

A *n*-order four variable refined theory is proposed to analyze the bending and free vibration of functionally graded plates. By dividing the transverse displacement into bending and shear components, the number of unknowns and governing equations of the present theory is reduced to four and is therefore less than alternate theories available in the scientific literature. The equations of motion derived from Hamilton principle are solved analytically for bending and free vibration problems of a simply supported plate. It is observed that the proposed higher order shear and normal deformation theory is not only accurate but also provides an elegant and easily implementable approach for simulating bending and vibration behaviors of FG plates, of relevance for example in spacecraft thermo-structural design. The formulation lends itself particularly well to finite element simulations (Curiel Sosa *et al*. 2012, 2013) and also other numerical methods employing symbolic computation for plate bending problems (Rashidi *et al*. 2012), which will be considered in the near future.

References

Abrate, S. (2006), "Free vibration buckling and static deflections of functionally graded plates", *Compos*. *Sci*. *Technol*., **66**(14), 2383-2394.

Bachir Bouiadjra, M., Houari, M.S.A. and Tounsi, A. (2012), "Thermal buckling of functionally graded plates according to a four-variable refined plate theory", *J*. *Therm*. *Stresses*, **35**(8), 677-694.

Batra, R.C. and Jin, J. (2005), "Natural frequencies of a functionally graded anisotropic rectangular plate", *J*. *Sound Vib*., **282**(1), 509-516.

Bodaghi, M. and Saidi, A.R. (2010), "Levy-type solution for bending analysis of thick functionally graded rectangular plates based on higher-order shear deformation plate theory", *Appl*. *Math*. *Model*., **34**(11), 3659-3670.

Bouderba, B., Houari, M.S.A. and Tounsi, A. (2013), "Thermomechanical bending response of FGM thick plates resting on Winkler-Pasternak elastic foundations", *Steel Compos*. *Struct*., *Int*. *J*., **14**(1), 85-104.

Bourada, M., Tounsi, A., Houari, M.S.A. and Adda Bedia, E.A. (2012), "A new four-variable refined plate theory for thermal buckling analysis of functionally graded sandwich plates", *J*. *Sandwich Struct*. *Mater*.,

14(1), 5-33.
Bouremana, M., Houari, M.S.A., Tounsi, A., Kaci, A. and Adda Bedia, E.A. (2013), "A new first shear deformation beam theory based on neutral surface position for functionally graded beams", *Steel Compos. Struct., Int. J.*, **15**(5), 467-479.
Chen, C.S., Fung, C.P. and Yu, S.Y. (2008), "The investigation on the vibration and stability of functionally graded plates", *J. Reinf. Plast. Compos.*, **27**(13), 1435-1447.
Chen, C.S., Hsu, C.Y. and Tzou, G.J. (2009), "Vibration and stability of functionally graded plates based on a higher order deformation theory", *J. Reinf. Plast. Compos.*, **28**(10), 1215-1234.
Chi, S.H. and Chung, Y.L. (2006a), "Mechanical behavior of functionally graded material plates under transverse load. Part I: Analysis", *Int. J. Solid. Struct.*, **43**(13), 3657-3674.
Chi, S.H. and Chung, Y.L. (2006b), "Mechanical behavior of functionally graded material plates under transverse load. Part II: Numerical results", *Int. J. Solid. Struct.*, **43**(13), 3675-3691.
Curiel Sosa, J.L., Munoz, J.J., Pinho, S.T. and Anwar Bég, O. (2012), "(XFEM) Simulation of damage in laminates", *Applied Sciences and Engineering* (*ECCOMAS 2012*), (J. Eberhardsteiner *et al*. Eds.), Vienna, Austria, September.
Curiel Sosa, J.L., Anwar Bég, O. and Liebana Murillo, J.M. (2013), "Finite element analysis of structural instability using a switching implicit-explicit technique", *Int. J. Comp. Method. Eng. Sci. Mech.*, **14**(5), 452-464.
Fahsi, B., Kaci, A., Tounsi, A. and Adda Bedia, E.A. (2012), "A four variable refined plate theory for nonlinear cylindrical bending analysis of functionally graded plates under thermomechanical loadings", *J. Mech. Sci. Tech.*, **26**(12), 4073-4079.
Fekrar, A., El Meiche, N., Bessaim, A., Tounsi, A. and Adda Bedia, E.A. (2012), "Buckling analysis of functionally graded hybrid composite plates using a new four variable refined plate theory", *Steel Compos. Struct., Int. J.*, **13**(1), 91-107.
Hadji, L., Atmane, H.A., Tounsi, A., Mechab, I. and Adda Bedia, E.A. (2011), "Free vibration of functionally graded sandwich plates using four variable refined plate theory", *Appl. Math. Mech.*, **32**(7), 925-942.
Hosseini-Hashemi, S., Fadaee, M. and Atashipour, S.R. (2011a), "Study on the free vibration of thick functionally graded rectangular plates according to a new exact closed-form procedure", *Compos. Struct.*, **93**(2), 722-735.
Hosseini-Hashemi, S., Fadaee, M. and Atashipour, S.R. (2011b), "A new exact analytical approach for free vibration of Reissner–Mindlin functionally graded rectangular plates", *Int. J. Mech. Sci.*, **53**(1), 11-22.
Houari, M.S.A., Benyoucef, S., Mechab, I., Tounsi, A. and Adda Bedia, E.A. (2011), "Two variable refined plate theory for thermoelastic bending analysis of functionally graded sandwich plates", *J. Therm. Stresses*, **34**(4), 315-334.
Koizumi, M. (1997), "FGM activities in Japan", *Compos. Part B.*, **28**(1-2), 1-4.
Lü, C.F., Lim, C.W. and Chen, W.Q. (2009a), "Semi-analytical analysis for multi-directional functionally graded plates: 3-D elasticity solutions", *Int. J. Numer. Method. Eng.*, **79**(1), 25-44.
Lü, C.F., Lim, C.W. and Chen, W.Q. (2009b), "Exact solutions for free vibrations of functionally graded thick plates on elastic foundations", *Mech. Adv. Mater. Struct.*, **16**(8), 576-584.
Matsunaga, H. (2008), "Free vibration and stability of functionally graded plates according to a 2-D higher-order deformation theory", *Compos. Struct.*, **82**(4), 499-512.
Matsunaga, H. (2009), "Stress analysis of functionally graded plates subjected to thermal and mechanical loadings", *Compos. Struct.*, **87**(4), 344-357.
Ould Larbi, L., Kaci, A., Houari, M.S.A. and Tounsi, A. (2013), "An efficient shear deformation beam theory based on neutral surface position for bending and free vibration of functionally graded beams", *Mech. Based Des. Struct. Mach*, **41**(4), 421-433.
Rashidi, M.M., Shooshtari, A. and Anwar Bég, O. (2012), "Homotopy perturbation study of nonlinear vibration of Von Kármán rectangular plates", *Comput. Struct.*, **106/107**, 46-55.
Reddy, J.N. (2000), "Analysis of functionally graded plates", *Int. J. Numer. Method Eng.*, **47**, 663-684.
Shahrjerdi, A., Bayat, M., Mustapha, F., Sapuan, S.M. and Zahari, R. (2010), "Second-order shear

deformation theory to analyze stress distribution for solar functionally graded plates", *Mech. Based Des. Struct Mach.*, **38**(3), 348-361.
Sobhy, M. (2013), "Buckling and free vibration of exponentially graded sandwich plates resting on elastic foundations under various boundary conditions", *Compos. Struct.*, **99**, 76-87.
Suresh, S. and Mortensen, A. (1998), *Fundamentals of Functionally Graded Materials*, IOM Communications Ltd., London, UK.
Talha, M. and Singh, B.N. (2010), "Static response and free vibration analysis of fgm plates using higher order shear deformation theory", *Appl. Math. Model.*, **34**(12), 3991-4011.
Vel, S.S. and Batra, R.C. (2004), "Three-dimensional exact solution for the vibration of functionally graded rectangular plates", *J. Sound Vib.*, **272**(3-5), 703-730.
Xiang, S., Jin, Y.X., Bi, Z.Y., Jiang, S.X. and Yang, M.S. (2011), "A *n*-order shear deformation theory for free vibration of functionally graded and composite sandwich plates", *Compos. Struct.*, **93**(11), 2826-2832.
Yahoobi, H. and Feraidoon, A. (2010), "Influence of neutral surface position on deflection of functionally graded beam under uniformly distributed load", *World Appl. Sci. J.*, **10**(3), 337-341.
Yaghoobi, H. and Torabi, M. (2013), "Exact solution for thermal buckling of functionally graded plates resting on elastic foundations with various boundary conditions", *J. Therm. Stresses*, **36**(9), 869-894.
Yaghoobi, H. and Yaghoobi, P. (2013), "Buckling analysis of sandwich plates with FGM face sheets resting on elastic foundation with various boundary conditions: An analytical approach", *Meccanica*, **48**(8), 2019-2035.
Zenkour, A.M. (2006), "Generalized shear deformation theory for bending analysis of functionally graded plates", *Appl. Math. Model.*, **30**(1), 67-84.
Zhang, D.G. and Zhou, Y.H. (2008), "A theoretical analysis of FGM thin plates based on physical neutral surface", *Comput. Mater. Sci.*, **44**(2), 716-720.

CC